Vasopressin Regulates Extracellular Vesicle Uptake by Kidney Collecting Duct Cells

Citation for published version:
Oosthuyzen, W, Scullion, KM, Ivy, JR, Morrison, EE, Hunter, RW, Starkey Lewis, PJ, O'Duibhir, E, Street, JM, Caporali, A, Gregory, CD, Forbes, SJ, Webb, DJ, Bailey, MA & Dear, JW 2016, 'Vasopressin Regulates Extracellular Vesicle Uptake by Kidney Collecting Duct Cells', *Journal of the American Society of Nephrology*, vol. 27, no. 11, pp. 3345-3355. https://doi.org/10.1681/ASN.2015050568

Digital Object Identifier (DOI):
10.1681/ASN.2015050568

Published In:
Journal of the American Society of Nephrology

Vasopressin regulates extracellular vesicle uptake by kidney collecting duct cells

Authors: Wilna Oosthuyzen[1], Kathleen M Scullion[1], Jessica R. Ivy[1], Emma E Morrison[1], Robert W Hunter[1], Philip J Starkey Lewis[2], Eoghan O'Duibhir[2], Jonathan M. Street[3], Andrea Caporali[1], Christopher D. Gregory[4], Stuart J Forbes[2], David J. Webb[1], Matthew A. Bailey[1] and James W. Dear[1 *]

Affiliation: 1. Pharmacology, Therapeutics and Toxicology, University of Edinburgh /BHF Centre for Cardiovascular Science, The Queen's Medical Research Institute, 47 Little France Crescent, Edinburgh EH16 4TJ. UK.

2. MRC Centre for Regenerative Medicine, Scottish Centre for Regenerative Medicine, 5 Little France Drive, Edinburgh EH16 4UU, UK.

3. Renal Diagnostics and Therapeutics Unit, National Institute of Diabetes and Digestive and Kidney Diseases, National Institutes of Health, Bethesda, Maryland, USA.

4. MRC/University of Edinburgh Centre for Inflammation Research, The Queen's Medical Research Institute, 47 Little France Crescent, Edinburgh EH16 4TJ. UK

*Corresponding author: James W. Dear
University/BHF Centre for Cardiovascular Science
University of Edinburgh
The Queen's Medical Research Institute
47 Little France Crescent
Edinburgh
EH16 4TJ
james.dear@ed.ac.uk
(+44) 0131 242 9216

Keywords: extra-cellular vesicles, vasopressin, kidney, exosomes
Short title: Vasopressin regulates vesicle uptake

Abstract

Extracellular vesicles (ECVs) are a novel route of inter-cellular communication along the nephron, with the potential to change the function of the recipient cell. However, it is not known whether this is a regulated process analogous to other signalling systems. Here we report that desmopressin, an analogue of the hormone vasopressin, stimulated fluorescently-loaded ECV uptake into a kidney collecting duct cell line ($mCCD_{C11}$) and into primary cells. To confirm uptake of biologically active ECVs we exposed $mCCD_{C11}$ cells to ECVs isolated from cells over-expressing the microRNA miR-503. In these cells, miR-503 target gene expression was down-regulated, but only in the presence of desmopressin. Mechanistically, ECV entry into $mCCD_{C11}$ cells required cyclic AMP production, was reduced by inhibiting dynamin, and was selective for ECVs from kidney tubular cells. To establish *in vivo* relevance we measured the urinary excretion and tissue uptake of fluorescently-loaded ECVs delivered systemically to mice before and after administration of the V2 receptor antagonist, tolvaptan. Basally, 2.5% of ECVs were recovered in the urine; tolvaptan increased recovery 5-fold and reduced ECV deposition in kidney tissue. Furthermore, in a patient with central diabetes insipidus, desmopressin reduced the excretion of ECVs derived from glomerular and proximal tubular cells. These data are consistent with vasopressin-regulated uptake of ECVs *in vivo*. We conclude that ECV uptake is a specific and regulated process. Physiologically, ECVs are a new mechanism of inter-cellular communication; therapeutically, ECVs represent a vehicle by which RNA therapy could be targeted to specific cells for the treatment of kidney disease.

Word count: 250/250

Introduction

Most, if not all, cell types release membrane-bound vesicles which can be isolated from biofluids such as blood[1], saliva[2] and urine.[3] These extra-cellular vesicles (ECVs) are heterogeneous, but can be broadly classed as being derived directly from the cell membrane or originating from intra-cellular pathways. Cell membrane derived ECVs include microparticles and apoptotic bodies. Classically, exosomes are distinguished from other ECV sub-populations by their unique biogenesis in the intra-cellular endosomal pathway following fusion of the multi-vesicular body with the limiting plasma membrane. These intra-cellular vesicles are termed exosomes after release into the extra-cellular space.

Conventionally, ECVs were viewed as a removal system for senescent or excess lipid and protein from cells.[4] Their cargo changes with cell injury and disease, so ECVs represent a potential reservoir for biomarker discovery, even a noninvasive replacement for tissue biopsy.[5] However, this promise has not yet been translated into a biomarker with real-life clinical utility. Research has identified a potential role in inter-cellular signalling - ECVs can deliver functional protein and RNA from one cell to another *in vitro*.[6] The mechanisms by which target cells internalise ECVs are yet to be fully elucidated and whether ECV transfer between cells occurs *in vivo* is still to be unequivocally confirmed. In cell culture studies, ECV uptake by cells has been reported via a number of mechanisms including clathrin-dependent endocytosis, caveolae-dependent endocytosis, phagocytosis and macropinocytosis.[7] However, it is not established whether ECV uptake by recipient cells is a physiologically regulated process and, if it is, which pathways or hormones are involved.

Urine contains ECVs originating from the circulation and from cells that line the urinary tract.[3] These ECVs maintain urine sterility by virtue of their antibacterial activity.[8] The most studied urinary ECV sub-type are exosomes, which are derived from the kidney's glomerulus and all regions of the nephron. Urinary exosomes contain protein, messenger RNA (mRNA), microRNA and mitochondrial DNA that originates from kidney tubular cells.[3,9] Given the unidirectional flow of urine along the nephron, the kidney is anatomically designed for potential ECV transfer from proximal to distal nephron segments. In the kidney there is evidence of ECV signaling: exosomes from injured tubular cells transfer mRNA into fibroblasts resulting in cell activation and stem cell-derived exosomes protect against acute kidney injury by transfer of RNA.[10,11] Using aquaporin (AQP) membrane water channels to track ECV signaling we previously demonstrated ECV-mediated AQP transfer from stimulated to unstimulated collecting duct cells.[12]

Using a kidney collecting duct cell line ($mCCD_{C11}$), which responds robustly to aldosterone and vasopressin stimulation by transporting sodium and water, respectively, we have established and characterised a model of ECV release. These ECVs are exosome-like in their properties: they express archetypal exosomal proteins, such as tumor susceptibility gene 101 (TSG101), which localise to a density on a sucrose gradient that is characteristic of exosomes.[13] Transmission electron microscopy (TEM) and nanoparticle tracking analysis (NTA) confirm that this collecting duct cell line releases ECVs of exosome size and shape that express surface exosomal markers.[12,14] We have previously demonstrated that vasopressin, a pituitary neuropeptide that regulates water homeostasis, modulates the aquaporin 2 (AQP2) content of these ECVs *in vitro* and this regulation translates into rodent models and humans.[12,14] The aim of the present study was to investigate the role of vasopressin in the regulation of ECV uptake into the kidney collecting duct.

Results

Vasopressin stimulates ECV uptake by $mCCD_{C11}$ and primary collecting duct cells

ECVs of exosomal size were present in the supernatant from the $mCCD_{C11}$ cells, as we have previously reported (**supplementary figure 1**). Release of ECVs from $mCCD_{C11}$ cells was significantly increased following stimulation with the vasopressin analogue, desmopressin **(supplementary figure 2).** When the size distribution of ECVs was analysed by NTA the increase in ECV release induced by desmopressin corrresponded to release of ECVs in the size range 20-100nm, an exosomal size distribution. NTA is a light scatter microscopy method of tracking micro- and nanoparticles based on direct and real-time tracking of the particles' Brownian movement, which results in a description of the particle size and concentration distribution in a given solution. NTA can be used to count and size specific subgroups of nanoparticles using fluorescent antibodies against surface proteins, including ECVs derived from kidney cells in culture and in urine.[14] $mCCD_{C11}$ cell ECVs were successfully loaded with fluorescent Cell Tracker label and membrane disruption with QIAzol cell lysis reagent substantially reduced the NTA signal, consistent with fluorescent loading of membrane-bound ECVs (**supplementary figure 3**). Cell Tracker nanocrystals in PBS without any ECVs produced no NTA signal.

ECV uptake by $mCCD_{C11}$ cells was quantified by tracking fluorescence and by the cellular response to microRNA-loaded ECVs – two complementary approaches that report physical uptake and biological activity, respectively. ECVs, harvested from $mCCD_{C11}$ cells and loaded with fluorescent nanocrystals (Cell Tracker label), were applied to different $mCCD_{C11}$ cells grown in a confluent monolayer. Entry of ECVs into the recipient cell was observed under fluorescent microscopy (**figure 1**), the percentage of fluorescent cells was determined by FACS analysis and the concentration of ECVs remaining in the supernatant was measured by NTA. Incubation of the recipient cells with the vasopressin analogue, desmopressin, caused a time-dependent increase in the proportion of fluorescent cells (**figures 1 and 2A&B**). Significant ECV uptake occurred after 48 hours of desmopressin stimulation; shorter exposure times had no effect **(figure 2A).** This is comparable to the time course of desmopressin-induced ECV release **(supplementary figure 2)** and AQP2 expression in this cell line.[12] At concentrations similar to the physiological concentration of vasopressin,[15] 96 hours of desmopressin incubation approximately doubled the proportion of recipient cells taking up fluorescent ECVs (**figure 2C**). Consistent with this, the concentration of fluorescently-loaded ECVs remaining in the supernatant was significantly reduced by treatment with desmopressin (**figure 2D**). Tolvaptan; a selective V2 receptor antagonist, abolished the increase in ECV uptake induced by desmopressin (**figure 2E**), while OPC-21268, a V1 antagonist had no effect (desmopressin stimulated $mCCD_{C11}$ cells 23.2±5.2% vs desmopressin stimulated cells treated with OPC-21268 (1μM) 18.8±1.4%, n=3, p=0.5). Endothelin-1, a peptide which inhibits sodium transport in the collecting duct,[16] had no effect on ECV uptake by $mCCD_{C11}$ cells when applied alone, but physiologically antagonised the effect of desmopressin (**figure 2F**).

To complement and confirm the data from fluorescence-based ECV tracking we utilised ECVs loaded with a specific microRNA and used cellular target mRNA suppression as the readout of functional ECV uptake. ECVs were harvested from a human umbilical vein endothelial cell (HUVEC) line transduced to over-express miR-503[18] and a control cell HUVEC line. This cell line was chosen as the mRNA targets of miR-503 are well-described.[18,19] The expression of miR-503 in the isolated ECV pellet was confirmed by qPCR (overexpressing Ct value 26.6 vs control Ct value >35). ECVs from both cell lines were added to unstimulated or desmopressin-stimulated $mCCD_{C11}$ cells . Target genes influenced by miR-503 have been identified: we measured the mRNA expression of VEGF-A, FGF2, CDC25A and CCNE1. ECVs containing miR-503 induced a significant down-regulation of the target genes following desmopressin stimulation (**figure 3**). In the absence of desmopressin there was no significant change in gene expression.

Building on these data from our collecting duct cell line, ECV uptake was visualised by fluorescence microscopy in rat primary collecting duct cells to determine whether ECV uptake was also regulated by the vasopressin system in native cells. We isolated cells expressing AQP2 from whole rat kidney **(figure 4).** There was uptake of ECVs into these cells, but only in the presence of desmopressin (3.16ng/ml for 2 hours) **(figure 4).**

cAMP and dynamin mediate desmopressin-induced ECV uptake

The V2 receptor is coupled with Gs proteins and causes activation of the cAMP pathway.[15] Inhibition of cAMP-dependent protein kinase A (PKA) with H-89 prevented the increase in uptake of fluorescent ECVs following desmopressin stimulation (**figure 5A**). Stimulation of $mCCD_{C11}$ cells with forskolin increased uptake of fluorescent ECVs independent of desmopressin stimulation (**figure 5B**). Endocytosis can be cAMP dependent[20] and, taken together with previous studies showing that ECVs enter cells through the endocytotic pathway[7], we investigated the role of dynamin, a GTPase that mediates endocytosis. Dynasore, a non-competitive inhibitor of dynamin activity[21,22], significantly reduced desmopressin-stimulated ECV uptake to a level below that of control cells (**figure 5C**). In combination, these data indicate that basal and desmopressin-induced uptake of ECVs requires cAMP activation and dynamin activity.

ECV uptake by $mCCD_{C11}$ cells is selective for ECV cell of origin

Next, we determined whether ECVs derived from different cell types are also internalised under vasopressin regulation. We incubated $mCCD_{C11}$ cells (without and with desmopressin stimulation) with equal numbers of ECVs (1×10^8 / mL) harvested from the following renal cell types: $mCCD_{C11}$ cells (mouse); proximal tubule (HK2 - human); and juxtaglomerular (RG1 - mouse). The ECVs from all cell types had similar size distributions, as quantified by NTA (**figure 6A**). Treating recipient $mCCD_{C11}$ cells with desmopressin increased uptake of the proximal tubule and collecting duct-derived ECVs but not of those from juxtaglomerular cells (**figure 6B**). This tubular cell selectivity was confirmed by NTA analysis, which demonstrated decreased proximal and collecting duct ECVs in the $mCCD_{C11}$ cell culture supernatant, but no change in ECVs from juxtaglomerular cells (**figure 6C**).

The V2 receptor is expressed on the basolateral membrane of the renal principal cell. Therefore we examined ECV uptake in $mCCD_{C11}$ cells polarised by growing on transwell plates and stimulated with desmopressin on either the apical or basolateral side. Basolateral desmopressin stimulated uptake of apically applied ECVs, whereas desmopressin applied to the apical membrane had no effect **(figure 6D).**

Vasopressin regulates urinary ECV excretion in mice and humans

As a control, mice were intravenously injected with ECV-free Cell Tracker nanocrystals in solution and there was no signal detected in their urine by NTA. Mice were intravenously injected with fluorescently-loaded ECVs derived from $mCCD_{C11}$ cells . The urinary excretion of these fluorescent ECVs was measured by NTA. QIAzol treatment of the urine substantially reduced the number of particles measured by NTA which is consistent with the presence of fluorescently-loaded membrane bound ECVs **(supplementary figure 4).**

Mice were then administered either tolvaptan, furosemide or vehicle (control) followed by a second injection of the same number of ECVs. Urine output increased 1.3 fold following tolvaptan and furosemide dose. In the control group, 2.5±1.0% and 1.8±0.7% of the systemically injected ECVs were recovered in the urine after the first and second ECV dose, respectively. In a separate group of mice, tolvaptan treatment increased the ECV excretion from 1.1±0.7% to 13.5±3.9%, consistent with inhibition of vasopressin-mediated ECV uptake (**figure 7A**) Treatment with furosemide produced no change in ECV excretion.

Kidney, liver and spleen tissue was examined by fluorescence microscopy after systemic injection of fluorescently-loaded ECVs without and with tolvaptan pre-treatment **(figure 8).** In the absence of tolvaptan ECVs were clearly present in kidney tissue (and liver and spleen).

After tolvaptan treatment there was a substantial reduction in ECV number in kidney, without an obvious effect on ECV deposition in liver and spleen **(figure 8).**

As an additional *in vivo* proof-of-concept study, the urinary excretion of nephron segment specific ECVs was measured in a patient with central diabetes insipidus using NTA combined with Qdot labelled antibodies for segment specific proteins.[14] Following self-directed desmopressin intra-nasal administration, there was a decrease in both glomerular (podocalyxin-like) and proximal tubular (cubilin) protein-expressing ECVs **(figure 7B).** This is consistent with our cell and mouse data and supports the presence of desmopressin-regulated uptake of glomerular and proximal tubule ECVs by distal segments of the nephron in humans.

Discussion

Extra-cellular vesicles (ECVs) transfer protein and RNA between cells to alter the phenotype of the recipient cell *in vitro*. Our data demonstrate that ECV uptake by recipient cells is hormonally regulated by vasopressin in kidney cell culture, mice and humans. We also demonstrate that ECVs can, by vasopressin-regulated transfer of microRNA, change gene expression profiles in the recipient $mCCD_{C11}$ cell. The renal tubular system is ideally suited to exploit this mechanism of cell-to-cell communication, which opens up a new paradigm for physiological cross-talk between nephron segments. Moreover, ECVs offer a vehicle for targeting RNA therapies to diseased kidney tubular cells.

Vasopressin is released from the posterior pituitary in response to an elevation in blood osmolality. Its principal role is to stimulate water reabsorption by the renal collecting duct. This is achieved through activation of the V2 receptor on the basolateral membrane of renal principal cells which, via a cAMP/PKA cascade, phosphorylates the water channel AQP2 permitting trafficking to the apical cell membrane from sub-apical recycling endosomes. In parallel, vasopressin stimulates endocytosis of vesicles from the cellular plasma membrane to maintain membrane equilibrium. In this paper, we demonstrate a new role for vasopressin as a hormonal regulator of ECV uptake in cells, mice and humans. In cell culture studies we used 4 complementary read-outs of ECV uptake – fluorescent microscopy, flow cytometry and microRNA transfer into cells, combined with NTA of ECVs remaining in the culture medium. The data generated by these different methodologies consistently demonstrated that desmopressin stimulated ECV uptake into $mCCD_{C11}$ cells and primary collecting duct cells. The time course of ECV uptake was different: $mCCD_{C11}$ cells needed 48h of desmopressin stimulation before significant uptake was recorded, similar to the time-frame required before desmopressin stimulates AQP2 expression and ECV release in these cells; by contrast, primary cells responded within 2h of exposure. One explanation for the different response times is that naïve $mCCD_{C11}$ cells require new protein production for uptake of ECVs, but this remains speculative. The uptake mechanism was V2 receptor-mediated and cAMP/PKA dependent, in keeping with the established physiological pathway that increases water uptake. In our cell model, desmopressin-induced ECV uptake was reduced by endothelin-1, suggesting that ECV uptake is under opposing physiological regulation by vasopressin and endothelin-1. This is consistent with data that indicate endothelin-1, via the ETB receptor, antagonizes the physiological actions of vasopressin in the collecting duct both *in vitro*[17] and *in vivo.*[16] Thus, the mechanism of vasopressin-induced ECV uptake is consistent with the known physiology of this hormone and is likely to be a consequence of hormone-induced plasma membrane endocytosis. Hormonal regulation of ECV entry into cells has not been demonstrated in any cell line and we also found that vasopressin stimulated ECV (likely exosome) release from $mCCD_{C11}$ cells. It is not yet clear how this up-take and release fits into a cell signalling paradigm and it is even possible that ECVs taken up from the tubular lumen could be re-released. Nevertheless, that both processes were influenced by vasopressin indicates that ECV inter-cellular signalling may be a tightly regulated physiological process.

There has been a substantial increase in publications on the biology of ECVs, particularly relating to their signalling potential. However, in the kidney and other organs there is little evidence that regulated signalling occurs *in vivo*. To test whether vasopressin is important for renal ECV uptake and excretion *in vivo* we injected fluorescently-loaded ECVs systemically into mice. After injection these ECVs appeared in urine and kidney tissue which is consistent with previous published studies[23] and important for two reasons. First, investigators performing proteomic and transcriptomic analysis of urinary ECVs cannot assume that new biomarkers have originated from the kidney, and urinary non-renal ECVs may offer a non-invasive way to assess the physiology and pathology on other (non-renal) organs. Second, the presence of plasma-derived ECVs in urine provides proof-of-concept that systemically administered novel therapeutic interventions, delivered within ECVs, could gain access to renal tubules. The mechanism of systemic ECV entry into urine remains to be determined and a greater understanding may allow ECV manipulation to increase their urinary excretion. We also demonstrated that tolvaptan, a selective V2 receptor antagonist, substantially increased the urinary excretion of systemically administered ECVs and reduced the number of ECVs present in kidney tissue. Furosemide had no effect despite increasing urine output, which strongly suggests that the increased excretion of ECVs following tolvaptan treatment was not due to the increased urine output *per se*. These are the first data that demonstrate vasopressin is a regulator of urinary ECV excretion and confirms that our findings in cells translate to mice. Combining antibodies to nephron segment-specific proteins with NTA can identify the cellular origin of urinary ECVs. We collected urine from a patient with central diabetes insipidus – a condition defined by lack of vasopressin - and determined the effect of intra-nasal desmopressin on glomerular and proximal tubule derived ECVs. Following desmopressin, the urinary concentration of these ECVs fell, which is consistent with vasopressin regulation of urinary ECV excretion in humans. While these human data are hypothesis-generating, they are entirely consistent with the data from cells and mice. A limitation is that the concentration of urinary creatinine changed as a result of desmopressin treatment making the normalisation of spot urine ECV numbers a challenge. In the future larger validation studies should be performed to confirm our human data. We conclude that kidney collecting duct cells, under the control of vasopressin, actively modify the population of ECVs in the urine. This is an important concept and must be accounted for in preclinical and clinical analysis of urinary ECV profiles.

Urine contains ECVs from multiple cell types outside and within the urinary tract. The collecting duct, at the distal end of the tubular urine flow, is therefore exposed to ECVs from multiple cell types, which express a wide range of surface proteins. Intriguingly, uptake by our $mCCD_{C11}$ cell line was selective with regard to the ECV cell of origin. Proximal tubular ECVs (HK2 cells) and $mCCD_{C11}$ cell ECVs were internalised under desmopressin regulation. By contrast, uptake of ECVs derived from the kidney juxtaglomerular cell (RG1) was not desmopressin-sensitive, despite this being a mouse cell line. This observation was confirmed by flow cytometry of the cells and NTA of the supernatant. The ECVs were of a similar size profile, suggesting that the selectivity of vasopressin-regulated uptake is based on surface molecules within the ECV, such as proteins. Physiologically, the collecting duct would be exposed to proximal tubular ECVs in greater number than ECVs derived from juxtaglomerular cells and selective uptake may augment proximal to distal tubular signalling. Therapeutically, such selectivity could be a major advantage for harnessing ECVs as a drug delivery system, permitting precision targeting of therapy to treat segment-specific renal tubular disorders.

The cargo of ECVs includes proteins, mitochondrial DNA and RNA from their cell of origin. Across a range of cell types it has been reported that ECVs can transfer microRNA into a recipient cell and this can result in modulation of target mRNA. We utilised ECVs that contain miR-503 to demonstrate that desmopressin stimulation results in decreased target mRNA expression in $mCCD_{C11}$ cells . Urinary ECVs contain multiple RNA species so there is clear potential for signalling both within the kidney and from other organs to kidney tubular cells. However, recent reports have introduced a note of caution; Chevillet *et al.*[24] reported that the content of microRNA in naturally occurring ECVs is very low. Nevertheless, the therapeutic potential of ECVs is high. Our data suggest that ECVs injected intravenously can freely enter urine and could be engineered to deliver a complex package of RNA and protein that simultaneously targets multiple steps in an intra-cellular disease pathway.[19] These ECVs could be targeted to specific kidney cell types by manipulation of their surface markers and by hormonal activation of target cells.

In conclusion, the uptake of ECVs by kidney collecting duct cells is regulated by vasopressin via intra-cellular pathways that also mediate the increase in water permeability. Vasopressin regulation occurs in cell lines, primary cells, mice and possibly humans. This regulated uptake of ECVs can result in intra-cellular modulation of target mRNA species.

Physiologically, ECVs are a fundamental new mechanism of inter-cellular communication; therapeutically, ECVs represent a novel vehicle by which RNA therapy can be targeted to specific cells for the treatment of kidney disease.

Methods:

Cell Culture

The murine cell line ($mCCD_{C11}$) was a kind gift from Hans-Peter Gaeggeler and Bernard Rossier (University of Lausanne, Lausanne, Switzerland)[25] and was grown as per Street *et al.*[12] Briefly, $mCCD_{C11}$ cells were grown in Dulbecco's modified Eagles medium (DMEM)–F12 medium, 1:1 (Gibco, Paisley, UK), supplemented with 2% fetal calf serum (FCS; Invitrogen, Paisley, UK), 1× insulin transferrin selenium (ITS) solution (Gibco), 100 IU/ml penicillin and 100μg/ml streptomycin (Invitrogen, Paisley, UK), 50 pM dexamethasone (Sigma Aldrich, Gillingham, UK), 1 nM 3,3,5-triiodo-L-thyronine sodium salt (Sigma Aldrich) and 10 ng/ml epidermal growth factor (Sigma Aldrich). Passaging was achieved by two 10 min washes with 1 mM EDTA in Dulbecco's modified phosphate-buffered saline (DPBS) followed by incubation in trypsin EDTA solution (Lonza, Basel, Switzerland). The presence of ECVs in FCS would interfere with our study so, after confluency, cells were washed twice in DPBS and grown in serum-free media.

For the different cell type experiments, we used ECVs isolated from the supernatant of HK2 and RG1 cell lines. The HK2 cell line was a kind gift from Dr Kenneth Simpson (University of Edinburgh, United Kingdom). HK2 cells were grown following the same described method as for $mCCD_{C11}$ cells . The RG1 cell line was grown by supplementing 1:1 DMEM/F12 (Gibco) with 10 % heat-inactivated FCS, IFN-γ (Peprotech, London, UK) at 100 μg/ml, and 1 % ITS containing 1 mg/ml insulin, 0.55 ml/ml human transferrin and 0.5 μg/ml sodium selenite (Gibco, Paisley, UK). 1X glutamine, 1X penicillin/streptomycin (pen/strep, Life Technologies) and 1X antioxidants (Sigma Aldrich) were added to this, as well as 10μM Y-27632 (Tocris, Bristol, UK) and filtered. The cell culture supernatant was removed from either cell type at 70-80% confluency of the cell layer.

Human umbilical vein ECs (HUVECs) and human microvascular ECs (HMVECs) (both from Lonza) were grown in EGM-2 (EBM-2 medium supplemented with growth factors) and 2% fetal bovine serum (FBS) (Lonza). Lipofectamine RNAiMAX (Life Technologies) was used to transfect HUVECs with pre-miR-503 or pre-miR-control (50nM final concentration) according to the manufacturer's instructions.

Primary cortical collecting duct isolation

Male rat kidneys were placed in DMEM/Ham's F12 medium with Glutamax (Gibco) containing 10% foetal bovine serum (Gibco), 100 U/ml penicillin and 100 μg/ml streptomycin (Gibco). After the peri-renal fat was removed, the kidneys were decapsulated and the cortex macroscopically dissected. The cortex was incubated in serum-free isolation medium containing 1mg/ml collagenase I and IV (Sigma Aldrich) for 45 minutes at 37°C. The resultant solution was ground and serially sieved to a final filter size of 40µm. The filtered solution was centrifuged at 27 000*g* through a 48% Percoll gradient (Sigma Aldrich) and the highest band of 3-4 distinct bands was carefully removed. The matter contained within this band was washed, sieved and the cells were resuspended in DMEM/Hams's F12 media with glutamax containing: 5 µg/ml insulin, 50 nM dexamethasone, 10 ng/ml epidermal growth factor, 5 µg/ml transferrin, 30 nM sodium selenite, 10 nM triiodothyronine, 100 U/ml penicillin, 100 µg/ml streptomycin, 25 mM $NaHCO_3$ and 10% FBS. The suspension was plated onto collagen-coated 35-mm tissue culture dishes (Corning) and maintained in an incubator under humidified 5% CO_2 atmosphere at 37°C.

Isolation and fluorescent loading of ECVs

Culture medium from the cells was vigorously vortexed then centrifuged at 15,000 x *g* for 10 min to pellet any cells, large membrane fragments and other debris. The supernatant was then centrifuged at 200,000 x *g* for 60 min to pellet ECVs. The pellet was washed with phosphate-buffered saline (PBS) and then re-centrifuged at 200,000 x *g* for 60 min before final suspension in PBS.[12]

Pelleted ECVs were loaded with Cell Tracker 655 (Invitrogen) following the manufacturer's protocol. Briefly, pelleted ECVs were incubated with the Cell Tracker 655 conjugate in 200ul fresh serum-free culture media for 1hour at 37°C. These labelled ECVs were washed with fresh media before being put back on confluent cells.

Collecting duct cell stimulation

Desmopressin (Sigma Aldrich) was added as per Street *et al.*[12] For short periods of stimulation, desmopressin and fluorescently-loaded ECVs were added together for 1-8 hours. With longer time periods of cell stimulation (24-96 hours), for the final 24 hours of stimulation fluorescent ECVs were added. At the end of the study the supernatant was collected for NTA analysis and cells removed by trypsinisation (as described previously[12]) for flow cytometry. In addition to desmopressin, in specific experiments for the final 24 hours the cells were treated with tolvaptan (10nM) (Sigma Aldrich), endothelin-1 (10pM) (Sigma Aldrich) or H-89 (25µM) (Sigma Aldrich).[26] Treatment with the Dynamin Inhibitor I (Dynasore (150uM): Sigma Aldrich) was for 45 minutes immediately prior to ECV addition, as per published studies.[22] Cells were treated with 10µM forskolin from *Coleus forskohlii* (Sigma Aldrich) and incubated with fluorescent ECVs overnight.[27,28] To polarise the $mCCD_{C11}$ cells they were cultured on the polyester membrane of Transwell inserts (Corning Costar Co, USA) at a high density to allow the cells to be confluent within three days. Desmopressin was added to the top or bottom Transwell chamber for 48 hours then fluorescent ECVs were added left to incubate for the final 24 hours of the 96 hour period.

Particle size and concentration distribution measurement with NTA

As per our published method[14], ECVs were analysed using the NanoSight LM 10 instrument (NanoSight Ltd, Amesbury, UK). The analysis settings were optimised and kept constant between samples and each video was analysed to give the mean, mode, median and estimated concentration for each particle size. All experiments were carried out at a 1:1000 dilution, yielding particle concentrations in the region of $1x10^8$ particles/ml in accordance with the manufacturer's recommendations. All samples were analysed in triplicate. For fluorescent NTA analysis a 532nm (green) laser diode excited the fluorescent loaded ECVs with a long pass filter (430nm).

For urine studies fluorescent labelling with antibody conjugated to Quantum dots was used with NTA. Anti-CD24 antibody was a kind gift of Dr. P. Altevogt, German Cancer Research Center, Heidelberg, Germany. Mouse anti-cubilin and anti-podocalyxin-like protein antibody was purchased from Abcam (Cambridge, UK) and Millipore (Billerica, MA, USA), respectively. Following the manufacturer's protocol, Qdots were conjugated to antibodies with a Qdot 605 Antibody Conjugation Kit (Invitrogen). For fluorescent NTA analysis a 532nm (green) laser diode excited the Qdots with a long pass filter (430nm) so that only fluorescent particles were tracked and labelled particle concentration determined by NTA software.

Flow cytometry for total cell fluorescence

Total cell fluorescence was measured by flow cytometry on a 5LSR Fortessa cytometer (BD Biosciences, Oxford, UK). Cells were briefly stained with 1µM DAPI nucleus stain (Sigma Aldrich) and having been exposed to Cell Tracker 655 (Invitrogen) labelled ECVs as described, was excited with a violet laser (405 nm) and emission detected using 450/50 and 630/70 band pass filters respectively. Gates were set using unstained cells and cells stained with DAPI alone. Flow cytometry data were analysed with FloJo LLC software version 8 (FlowJo LLC, Oregon, USA) and the results are presented as the percentage of total fluorescent cells.

Fluorescence microscopy

Using control and desmopressin-stimulated cells grown on a cover slip in a 35mm glassbottom dish or fixed mouse tissue, internalisation of labelled ECVs with DAPI stained $mCCD_{C11}$ cell nuclei and Phalloidin stained cell membranes (Sigma Aldrich) or AQP2 fluorescent antibodies (Merck Millipore, USA) was visualised by an Olympus AX-70 Provis epifluorescence microscope equipped with a Hamamatsu Orca II CCD camera. Images were collected with a 60 x oil immersion objective lens and acquired by using mDaemon software (Zenn, Manchester, UK). Each picture was acquired with laser intensities and amplifier gains adjusted to avoid pixel saturation and analysed using Adobe Photoshop CC 2014 (Adobe Systems, San Jose, California).

Transmission electron microscopy of $mCCD_{C11}$ cell culture supernatant was performed as previously described (2).

RNA extraction and quantitative real time analysis

Total RNA was extracted using miReasy kit (Qiagen, Venlo, Netherlands). Real-time quantification to measure microRNAs was performed with the TaqMan microRNA reverse transcription kit and microRNA assay (miR-503) (Applied Biosystems, Life Technologies) with Lightcycler 480 (Roche Diagnostics, Penzberg, Germany). SYBR qPCR was used to measure vascular endothelial growth-factor A (VEGF-A), fibroblast growth factor-2 (FGF2), cell division cycle 25A (CDC25A), cyclin-1E (CCNE1) and 18S rRNA. Primers are pre-designed from Sigma (KiCqStart^{TM} Primers). Each reaction was performed in triplicate. Quantification was performed by the 2ΔΔCt method.[29]

Animals

All experiments were conducted in accordance with UK Home Office regulations and the Animals (Scientific Procedures) Act 1986. Wild type (C57BL6/J and CD1) mice were sex and age matched across experiments. General anaesthesia was induced by intra-peritoneal injection of 100mg/kg thiobutabarbital sodium and venous access gained via the jugular vein. Urine flow was maintained throughout with a 0.9% saline infusion (0.2mL/10gbw/hour i.v). A bolus of cell tracker labelled ECVs from $mCCD_{C11}$ cells was injected in a final volume of 0.1ml (i.v.). Urine was collected via a urinary catheter for 2 hours following injection. The injection of ECVs was repeated without or with preceding tolvaptan administration (0.3mg/kg i.v) or furosemide (1mg/kg, i.v.).

Clinical case study

Repeated urine samples were obtained from a 16-year-old male with stable central diabetes insipidus (CDI) secondary to a craniopharyngioma, who was being routinely treated with daily desmopressin (dDAVP nasal spray; 0.1ml (10mcg) desmopressin acetate per spray).

The CDI patient samples were initially stored at 4°C then frozen at -80 °C. Analysis of the CDI patient samples were performed by a researcher blinded to the timing of desmopressin treatment. The protocol was agreed by the institutional ethical review body and informed consent was obtained.

Statistical analysis

Unless otherwise indicated, analyses were performed on data generated from triplicate results. Data were analysed using GraphPad Prism Version 6 (GraphPad Software, La Jolla, CA, USA). From the NTA data, the area under the curve (AUC) was determined following the trapezoidal rule for particles sized 20-100nm. Flow cytometry data were analysed using FloJo LLC, version 8 (FloJo LLC) gating around the main cell population. Total cell fluorescence was determined as the median of single cells lying in a gate defined proportioned from the unstained control, in a forward scatter vs. side scatter dot plot, expressed as percentage total cell fluorescence. Non-parametric Kolmogorov-Smirnov t tests and ANOVAs were used to determine significant differences between different conditions. A value of $p < 0.05$ was the level of nominal significance.

Acknowledgements

WO was funded by a grant from the Diabetes Research & Wellness Foundation; JRI by a British Heart Foundation PhD studentship (FS/11/78/29328). Author JWD acknowledges the support of NHS Research Scotland (NRS) through NHS Lothian. All the authors acknowledge the contribution of the BHF Centre of Research Excellence Award (RE/08/001) and the UK Regenerative Medicine Platform Niche Hub.

Author Contributions

Experiments were designed and performed by WO with assistance from KMS, JRI, JMS, EEM and RWH. Supervision was by JWD and MAB, supported by PJSL, EO, AC, SJF, CDG and DJW. All authors contributed to writing the manuscript.

Competing Financial Interests

None

References

1. Caby, M.-P., Lankar, D., Vincendeau-Scherrer, C., Raposo, G. & Bonnerot, C. Exosomal-like vesicles are present in human blood plasma. *Int. Immunol.* **17,** 879–887 (2005).
2. Lässer, C. *et al.* Human saliva, plasma and breast milk exosomes contain RNA: uptake by macrophages. *J. Transl. Med.* **9,** 9 (2011).
3. Pisitkun, T., Shen, R.-F. & Knepper, M. A. Identification and proteomic profiling of exosomes in human urine. *Proc. Natl. Acad. Sci. U. S. A.* **101,** 13368–13373 (2004).
4. Vlassov, A. V., Magdaleno, S., Setterquist, R. & Conrad, R. Exosomes: Current knowledge of their composition, biological functions, and diagnostic and therapeutic potentials. *Biochim. Biophys. Acta BBA - Gen. Subj.* **1820,** 940–948 (2012).
5. Bramham, K., Mistry, H. D., Poston, L., Chappell, L. C. & Thompson, A. J. The non-invasive biopsy—will urinary proteomics make the renal tissue biopsy redundant? *QJM Int. J. Med.* **102,** 523–538 (2009).
6. Valadi, H. *et al.* Exosome-mediated transfer of mRNAs and microRNAs is a novel mechanism of genetic exchange between cells. *Nat. Cell Biol.* **9,** 654–659 (2007).
7. Tian, T. *et al.* Dynamics of exosome internalization and trafficking. *J. Cell. Physiol.* **228,** 1487–1495 (2013).
8. Hiemstra, T. F. *et al.* Human urinary exosomes as innate immune effectors. *J. Am. Soc. Nephrol. JASN* **25,** 2017–2027 (2014).
9. Alvarez, M. L., Khosroheidari, M., Ravi, R. K. & DiStefano, J. K. Comparison of protein, microRNA, and mRNA yields using different methods of urinary exosome isolation for the discovery of kidney disease biomarkers. *Kidney Int.* **82,** 1024–1032 (2012).
10. Borges, F. T. *et al.* TGF-β1–Containing Exosomes from Injured Epithelial Cells Activate Fibroblasts to Initiate Tissue Regenerative Responses and Fibrosis. *J. Am. Soc. Nephrol.* **24,** 385–392 (2013).

11. Collino, F. *et al.* AKI Recovery Induced by Mesenchymal Stromal Cell-Derived Extracellular Vesicles Carrying MicroRNAs. J. Am. Soc. Nephrol. **26,** 2349-2360 (2015).

12. Street, J. M. *et al.* Exosomal transmission of functional aquaporin 2 in kidney cortical collecting duct cells. *J. Physiol.* **589,** 6119–6127 (2011).

13. Keller, S. *et al.* CD24 is a marker of exosomes secreted into urine and amniotic fluid. *Kidney Int.* **72,** 1095–1102 (2007).

14. Oosthuyzen, W. *et al.* Quantification of human urinary exosomes by nanoparticle tracking analysis. *J. Physiol.* **591,** 5833–5842 (2013).

15. Knepper, M. A. & Star, R. A. Vasopressin: friend or foe? *Nat. Med.* **14,** 14–16 (2008).

16. Kohan, D. E. The renal medullary endothelin system in control of sodium and water excretion and systemic blood pressure. *Curr. Opin. Nephrol. Hypertens.* **15,** 34–40 (2006).

17. Kohan, D. E. Biology of endothelin receptors in the collecting duct. *Kidney Int.* **76,** 481–486 (2009).

18. Caporali, A. *et al.* Deregulation of microRNA-503 Contributes to Diabetes Mellitus–Induced Impairment of Endothelial Function and Reparative Angiogenesis After Limb Ischemia. *Circulation* **123,** 282–291 (2011).

19. Zhou, B. *et al.* MicroRNA-503 targets FGF2 and VEGFA and inhibits tumor angiogenesis and growth. *Cancer Lett.* **333,** 159–169 (2013).

20. Musch, M. W. *et al.* Cyclic AMP-mediated endocytosis of intestinal epithelial NHE3 requires binding to synaptotagmin 1. *Am. J. Physiol. Gastrointest. Liver Physiol.* **298,** G203–211 (2010).

21. Macia, E. *et al.* Dynasore, a cell-permeable inhibitor of dynamin. *Dev. Cell* **10,** 839–850 (2006).

22. Kirchhausen, T., Macia, E. & Pelish, H. E. Use of dynasore, the small molecule inhibitor of dynamin, in the regulation of endocytosis. *Methods Enzymol.* **438,** 77–93 (2008).

23. Cheng, Y. *et al.* A translational study of urine miRNAs in acute myocardial infarction. *J. Mol. Cell. Cardiol.* **53,** 668–676 (2012).

24. Chevillet, J. R. *et al.* Quantitative and stoichiometric analysis of the microRNA content of exosomes. *Proc. Natl. Acad. Sci.* **111,** 14888–14893 (2014).

25. Gaeggeler, H.-P. *et al.* Mineralocorticoid versus glucocorticoid receptor occupancy mediating aldosterone-stimulated sodium transport in a novel renal cell line. *J. Am. Soc. Nephrol.* **16,** 878–891 (2005).

26. Gupta, I. R. *et al.* Protein Kinase A Is a Negative Regulator of Renal Branching Morphogenesis and Modulates Inhibitory and Stimulatory Bone Morphogenetic Proteins. *J. Biol. Chem.* **274,** 26305–26314 (1999).

27. Butterworth, M. B., Edinger, R. S., Johnson, J. P. & Frizzell, R. A. Acute ENaC Stimulation by cAMP in a Kidney Cell Line is Mediated by Exocytic Insertion from a Recycling Channel Pool. *J. Gen. Physiol.* **125,** 81–101 (2005).

28. Umenishi, F., Narikiyo, T., Vandewalle, A. & Schrier, R. W. cAMP regulates vasopressin-induced AQP2 expression via protein kinase A-independent pathway. *Biochim. Biophys. Acta BBA - Biomembr.* **1758,** 1100–1105 (2006).

29. Schmittgen, T. D. & Livak, K. J. Analyzing real-time PCR data by the comparative CT method. *Nat. Protoc.* **3,** 1101–1108 (2008).

Legends

Figure 1. Fluorescent microscopy of unstimulated (left) and desmopressin-stimulated (3.16ng/ml for 96 hours - right) mCCD$_{C11}$ cells incubated with fluorescently loaded ECVs (red). Desmopressin stimulated ECV uptake into the cellular cytoplasm. DAPI-stained nuclei (blue), cell membrane stained with phalloidin (green).

Figure 2. ECV uptake by mCCD$_{C11}$ cells is increased by desmopressin stimulation. A.) Flow cytometry data demonstrating no significant fluorescently-loaded ECV uptake following desmopressin stimulation (3.16ng/ml) for up to 8 hours (n=3). Fluorescent cells expressed as % of total cell number. B.) Flow cytometry data demonstrating ECV uptake following longer desmopressin stimulation. (n=3, * $p < 0.05$: 3.16ng/ml desmopressin stimulation vs no stimulation). C.) Desmopressin (3.16ng/ml for 96 hours) stimulated mCCD$_{C11}$ cells had significantly increased fluorescence after incubation with labelled ECVs. Fluorescent cells expressed as % of total cell number (n=5). D.) NTA analyses of fluorescently-loaded ECVs in the cell culture supernatant from control and desmopressin (3.16ng/ml for 96 hours) stimulated cells presented as the area under the concentration curve (AUC) for particles sized between 20-100nm (n=5). Desmopressin stimulation reduced the concentration of ECVs in the supernatant. E.) Fluorescence of control and desmopressin stimulated cells (3.16ng/ml for 96 hours) exposed to fluorescently-loaded ECVs in the absence and presence of tolvaptan (10nM). Fluorescent cells expressed as % of total cell number (n=5). F.) Fluorescence of control and desmopressin stimulated cells (3.16ng/ml for 96 hours) exposed to fluorescently-loaded ECVs in the absence and presence of endothelin-1 (10pg/mL). Fluorescent cells expressed as % of total cell number (n=5). Figures C-F are Tukey plots (bottom and top of the box are the first and third quartiles, and the band inside is the median. The whiskers are the lowest datum still within 1.5 IQR of the lower quartile and the highest datum still within 1.5 IQR of the upper quartile). * $p < 0.05$.

Figure 3. ECVs deliver functional microRNA into desmopressin-stimulated mCCD$_{C11}$ cells. Change in gene expression when desmopressin stimulation (3.16ng/ml for 96 hours) is compared to unstimulated cells in the absence of ECVs, with control HUVEC derived ECVs or with miR-503 loaded ECVs. A.) vascular endothelial growth factor-A (VEGF-A), B.) fibroblast growth-factor 2 (FGF2), C.) cyclin E-1 (CCNE1) and D.) cell division cycle 25A (CDC25A). Values are expressed as the difference between Ct values in unstimulated cells – Ct values in desmopressin stimulated cells with 18S as endogenous control. Negative values indicate down-regulation and positive values indicate up-regulation of target genes by desmopressin without or with the stated ECVs. n=9, * $p < 0.05$. All plots are Tukey plots.

Figure 4. Rat primary collecting duct cells take up ECVs after desmopressin stimulation. The cells express AQP2 protein (green), as detected by fluorescent antibody labelling. Fluorescently loaded ECVs (red) enter primary cells with desmopressin (3.16ng/ml for 2 hours) treatment. DAPI-stained nuclei are blue.

Figure 5. ECV uptake by $mCCD_{C11}$ cells following desmopressin stimulation is mediated by cAMP and dynamin activity. A.) Desmopressin (3.16ng/ml for 96 hours) stimulated ECV uptake which was decreased by PKA inhibition (H-89 – 25μM) of the cAMP pathway. B.) ECV uptake was increased by cAMP stimulation through forskolin (10μM). C.) Dynasore (150nM) inhibition of dynamin activity decreased ECV uptake by desmopressin stimulated cells below that of the control cells. In figures A-C: fluorescent cells expressed as % of total cell number. n= 6 * $p <0.05$. All plots are Tukey plots.

Figure 6. Cell type specificity for ECV uptake A.) NTA measurement of ECVs from different cell types prior to incubation with $mCCD_{C11}$ cells. CCD = collecting duct, HK2 = proximal tubule and RG1 = juxtaglomerular cell derived B.) Comparing total cell fluorescence between control and desmopressin (3.16ng/ml for 96 hours) stimulated $mCCD_{C11}$ cells following labelled ECV incubation from 3 cell types: $mCCD_{C11}$ cells (CCD), HK2 (human proximal tubular cell line) and RG1 (murine juxtaglomerular cell line). 1 x 10^8/mL ECVs were added to all experiments (n=6. * $p < 0.05$). C.) NTA analyses of cell culture supernatant incubated with different cell type derived ECVs ($mCCD_{C11}$, HK2 and RG1) from control and desmopressin (3.16ng/ml for 96 hours) stimulated cells presented as the area under the concentration curve (AUC) for particles sized between 20-100nm. Desmopressin stimulation reduced the concentration of $mCCD_{C11}$ and HK2 ECVs in the supernatant but not in cells incubated with RG1 ECVs D.) Polarised cells take up ECVs under desmopressin regulation. Total cell fluorescence of polarised $mCCD_{C11}$ cells stimulated with desmopressin (3.16ng/ml for 96 hours) either apically or basolaterally compared to unstimulated cells. Labelled ECVs were applied to apical compartment of Transwell (n=3. * $p < 0.05$). Figure B-D are Tukey plots.

Figure 7. Vasopressin V2 receptor regulates urinary ECV excretion in mice and humans. A.) Urinary excretion of systemically adminstered ECVs in mice. Group 1 – control group; urine ECV excretion following 2 i.v. injections of fluorescently-loaded ECVs. Group 2 – urine ECV excretion after 2 i.v. injections of labelled ECVs. Between injections mice were treated with tolvaptan (0.3mg/kg). n=5 per group, * $p < 0.05$. Group 3 – urine ECV excretion after 2 i.v. injections of labelled ECVs. Between injections mice were treated with furosemide

(1mg/kg, n=4). ECV excretion expressed as percentage of the total number of injected ECVs excreted in the urine. Data expressed as a Tukey plot. B.) 24 hour ECV excretion by a patient with central diabetes insipidus. Lines represent the time of desmopressin treatment (dashed line) and concentration of ECVs expressing nephron-segment specific proteins: glomerular (podocalyxin-like protein, PODX-L), proximal tubular (cubilin), and CD24 (pan-segment urinary ECV marker). ECV urine concentration measured by NTA and normalised by urinary creatinine concentration. All data are expressed as mean±SD. NTA measurements were taken in triplicate for each time point.

Figure 8. Tissue distribution of fluorescently-loaded ECVs systemically injected into mice without and with tolvaptan pre-treatment. After IV injection of ECVs mouse organs were harvested 1 hour later. Red = ECVs, blue = DAPI, green = AQP2. Without tolvaptan red signal is present in kidney tissue. With tolvaptan (0.3mg/kg) pretreatment the red signal is reduced. ECVs are present in liver and spleen without and with tolvaptan. Bar, 20μm.

Supplementary figure 1. Structures of exosome size and shape are visible in the $mCCD_{C11}$ cell culture medium using transmission electron microscopy. Bar, 100 nm.

Supplementary figure 2. ECVs of exosome size are released from $mCCD_{C11}$ cells following stimulation by desmopressin. A) Number of particles in the supernatant from $mCCD_{C11}$ cells stimulated with desmopressin (3.16ng/ml) for the time indicated. Particles measured by NTA. Data are presented as the area under the concentration curve (AUC) for particles sized between 20-100nm. n=5. *p=0.02. B) Number of particles in the supernatant from $mCCD_{C11}$ cells stimulated with desmopressin (3.16ng/ml) for the time indicated. Particles measured by NTA. Data are presented as the area under the concentration curve (AUC) for particles sized between 100-500nm. n=5.

Supplementary figure 3. Kidney collecting duct cell ECVs were loaded with fluorescent Cell Tracker label and had an exosomal size distribution, as measured by NTA (A). Membrane disruption with QIAzol cell lysis reagent substantially reduced this NTA signal, consistent with fluorescent loading of membrane-bound ECVs (B).

Supplementary figure 4. Particles of exosome size are present in mouse urine after intravenous injection of fluorescently-loaded ECVs derived from $mCCD_{C11}$ cells. Treatment of the urine with QIAzol cell lysis reagent substantially reduced this NTA signal, consistent with the presence of fluorescently-loaded membrane-bound ECVs. A). NTA trace demonstrating particle size and concentration. B) Tukey plot of urine before and after QIAzol treatment. Data are presented as the area under the concentration curve (AUC) for particles sized between 20-100nm. n=5. *$p<0.05$.

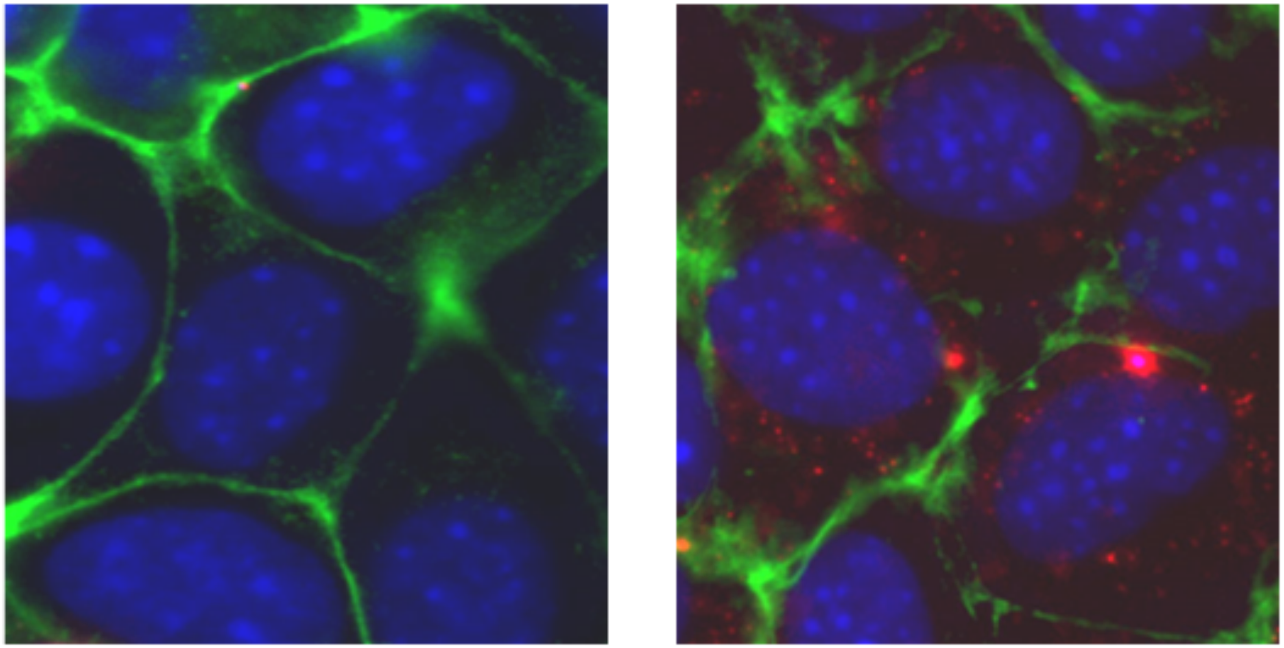

Figure 1

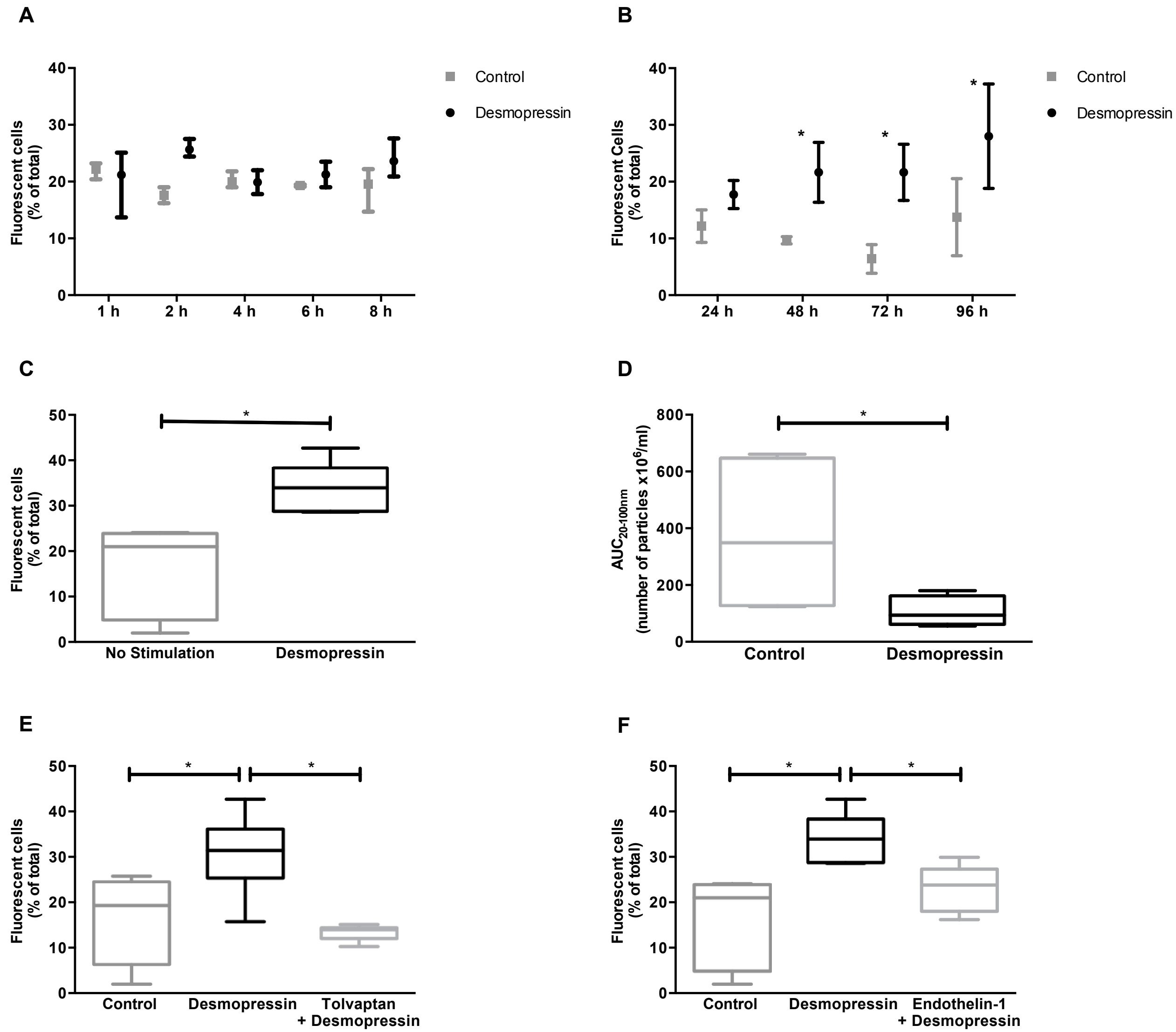
A
Fluorescent cells
(% of total)
0
10
20
30
40
1 h
2 h
4 h
6 h
8 h
Control
Desmopressin
B
Fluorescent Cells
(% of total)
24 h
48 h
72 h
96 h
*
Control
Desmopressin
C
Fluorescent cells
(% of total)
50
No Stimulation
Desmopressin
D
AUC20-100nm
(number of particles x10^6/ml)
0
200
400
600
800
Control
Desmopressin
E
Fluorescent cells
(% of total)
Control
Desmopressin
Tolvaptan
+ Desmopressin
F
Fluorescent cells
(% of total)
Control
Desmopressin
Endothelin-1
+ Desmopressin

Figure 2

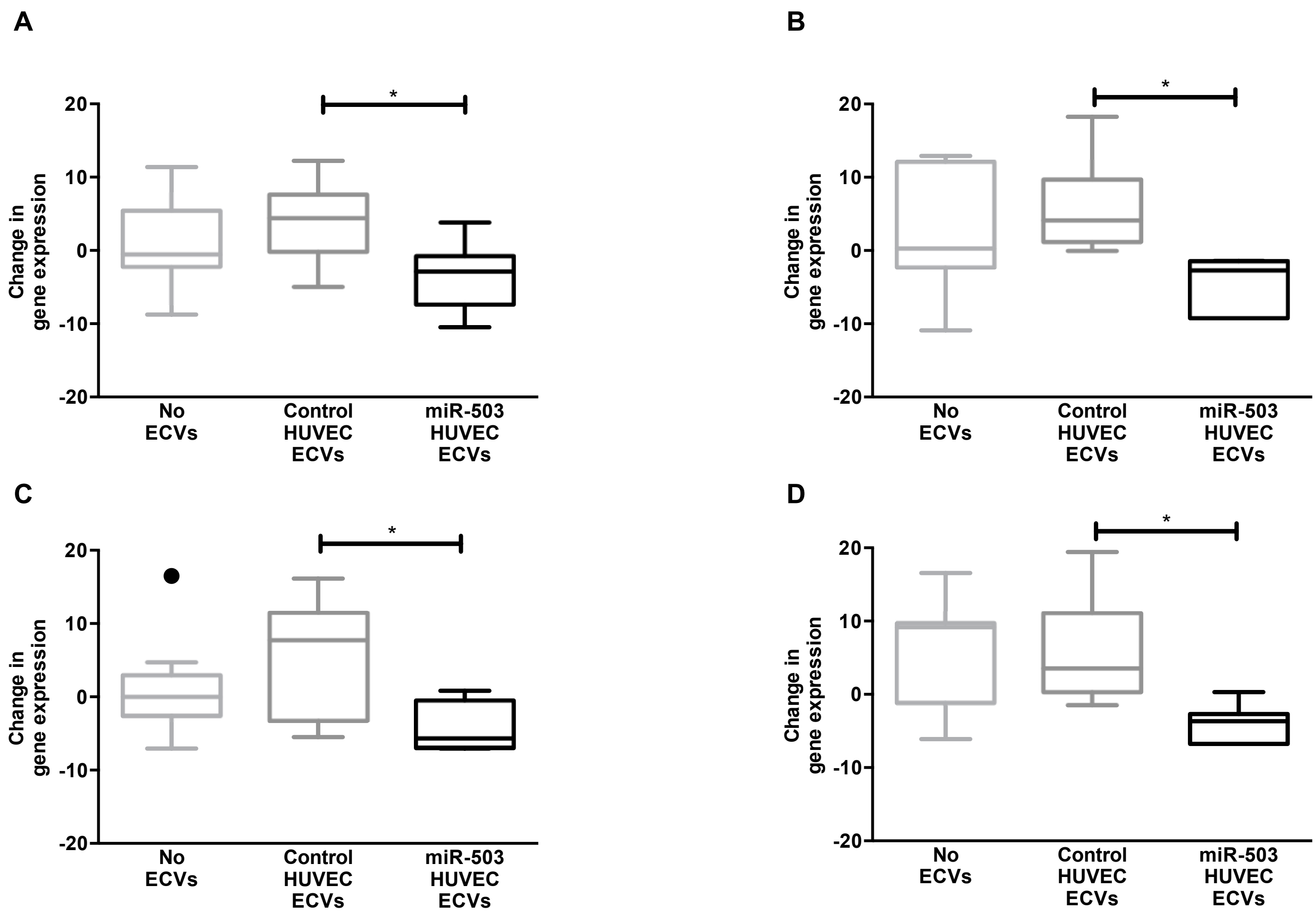
A
B
C
D
*
20
10
0
-10
-20
Change in
gene expression
No
ECVs
Control
HUVEC
ECVs
miR-503
HUVEC
ECVs

Figure 3

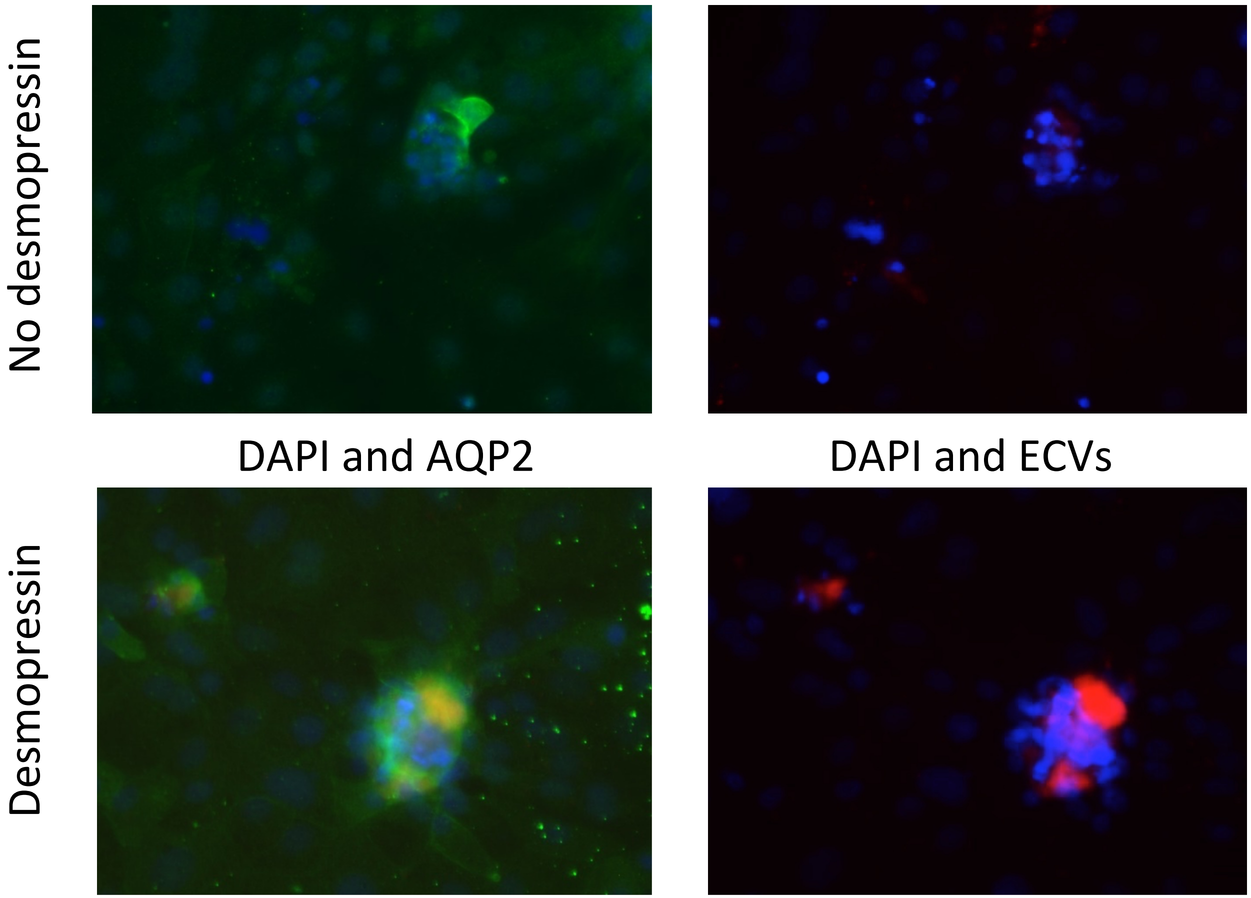

Figure 4

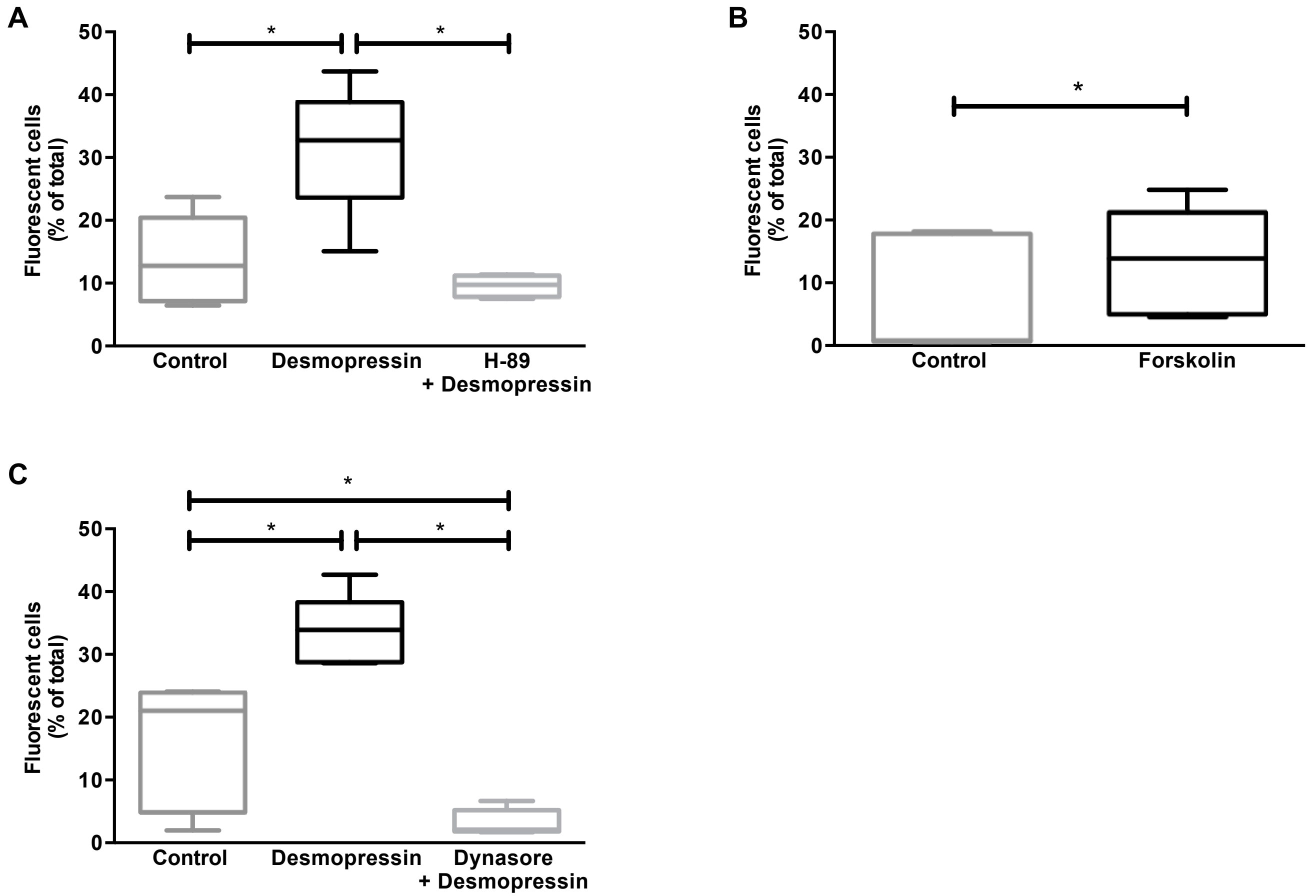
A
B
C
Fluorescent cells
(% of total)
0
10
20
30
40
50
*
Control
Desmopressin
H-89
+ Desmopressin
Forskolin
Dynasore
+ Desmopressin

Figure 5

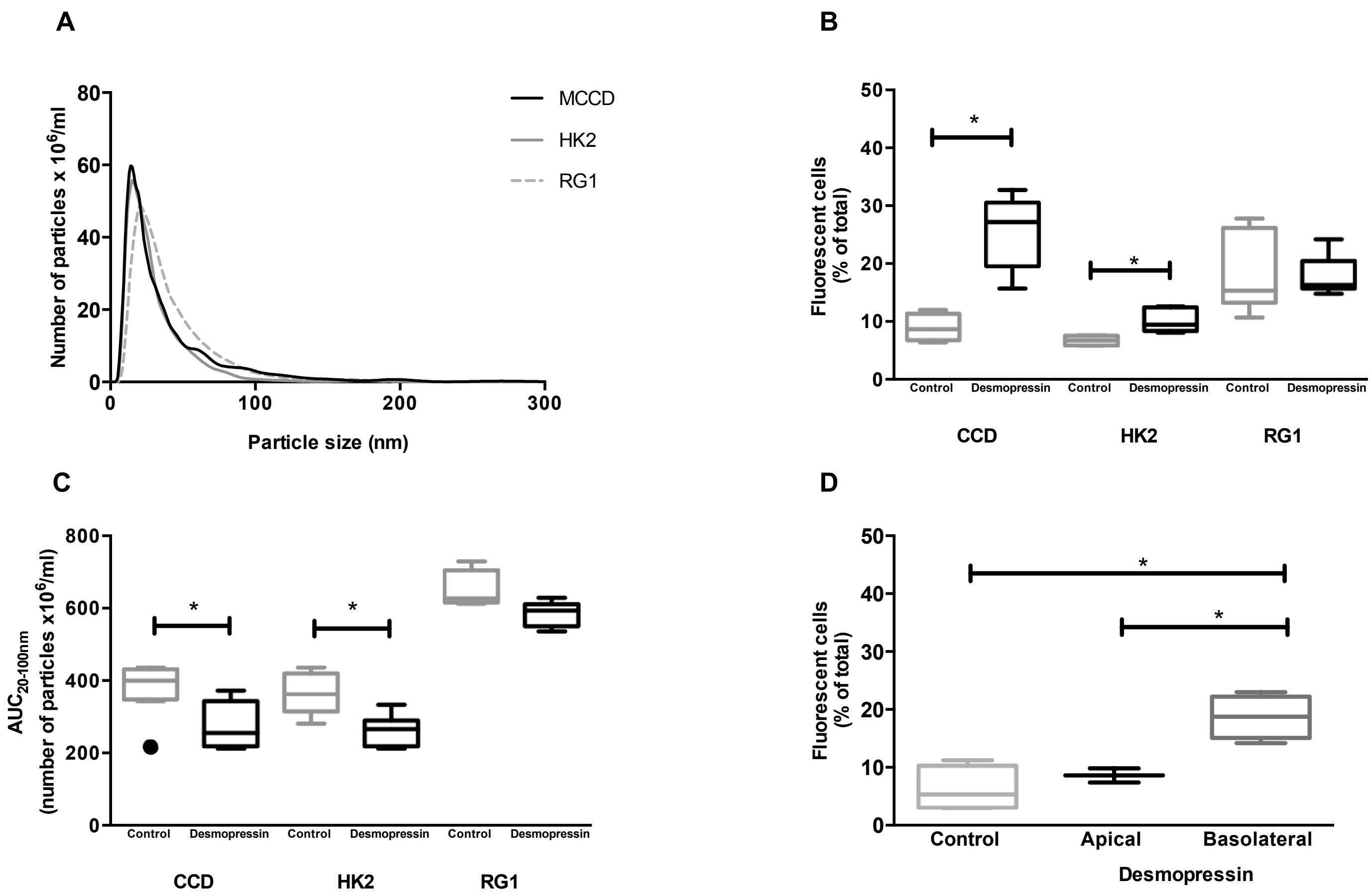
A
B
C
D
MCCD
HK2
RG1
Number of particles x 10^6/ml
Particle size (nm)
Fluorescent cells (% of total)
Control
Desmopressin
CCD
HK2
RG1
$AUC_{20-100nm}$ (number of particles x10^6/ml)
Apical
Basolateral
Desmopressin

Figure 6

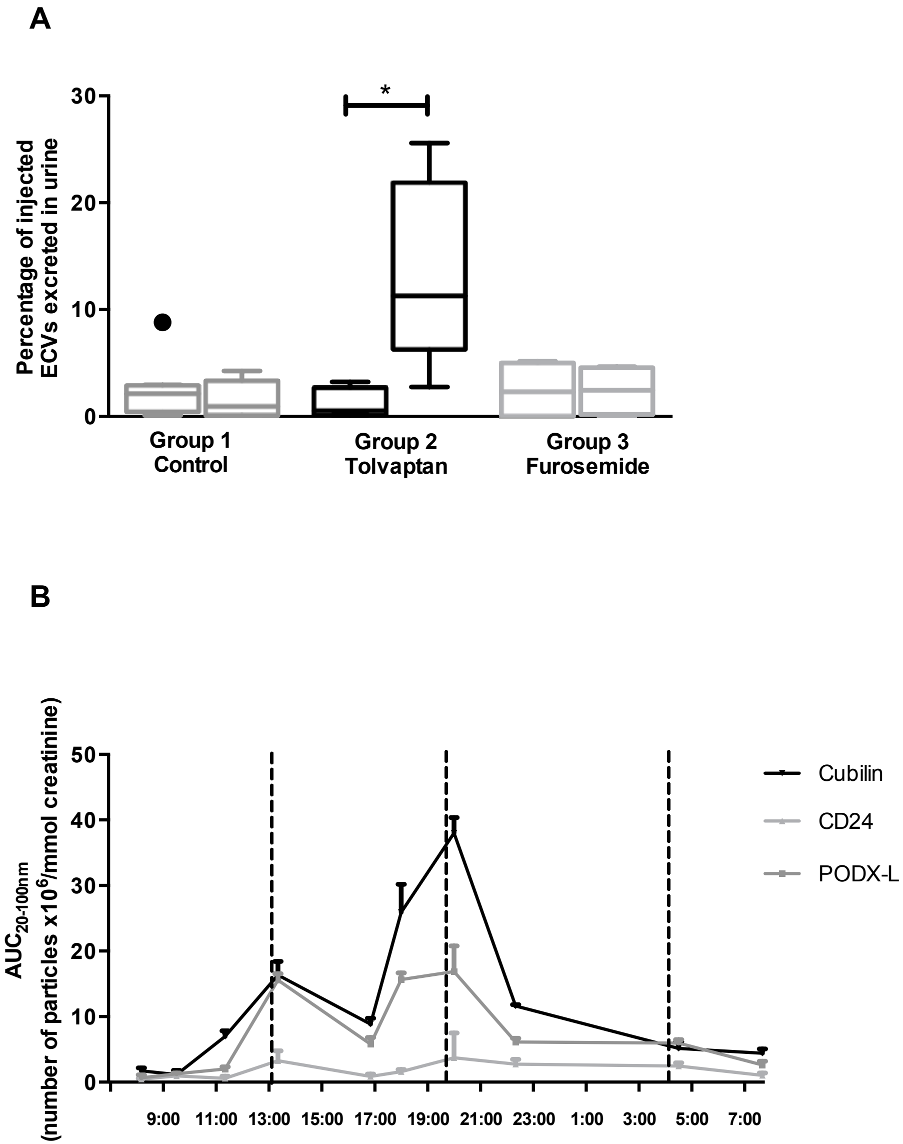
A
Percentage of injected ECVs excreted in urine
30
20
10
0
*
Group 1
Control
Group 2
Tolvaptan
Group 3
Furosemide
B
AUC20-100nm
(number of particles x10^6/mmol creatinine)
50
40
30
20
10
0
9:00
11:00
13:00
15:00
17:00
19:00
21:00
23:00
1:00
3:00
5:00
7:00
Cubilin
CD24
PODX-L

Figure 7

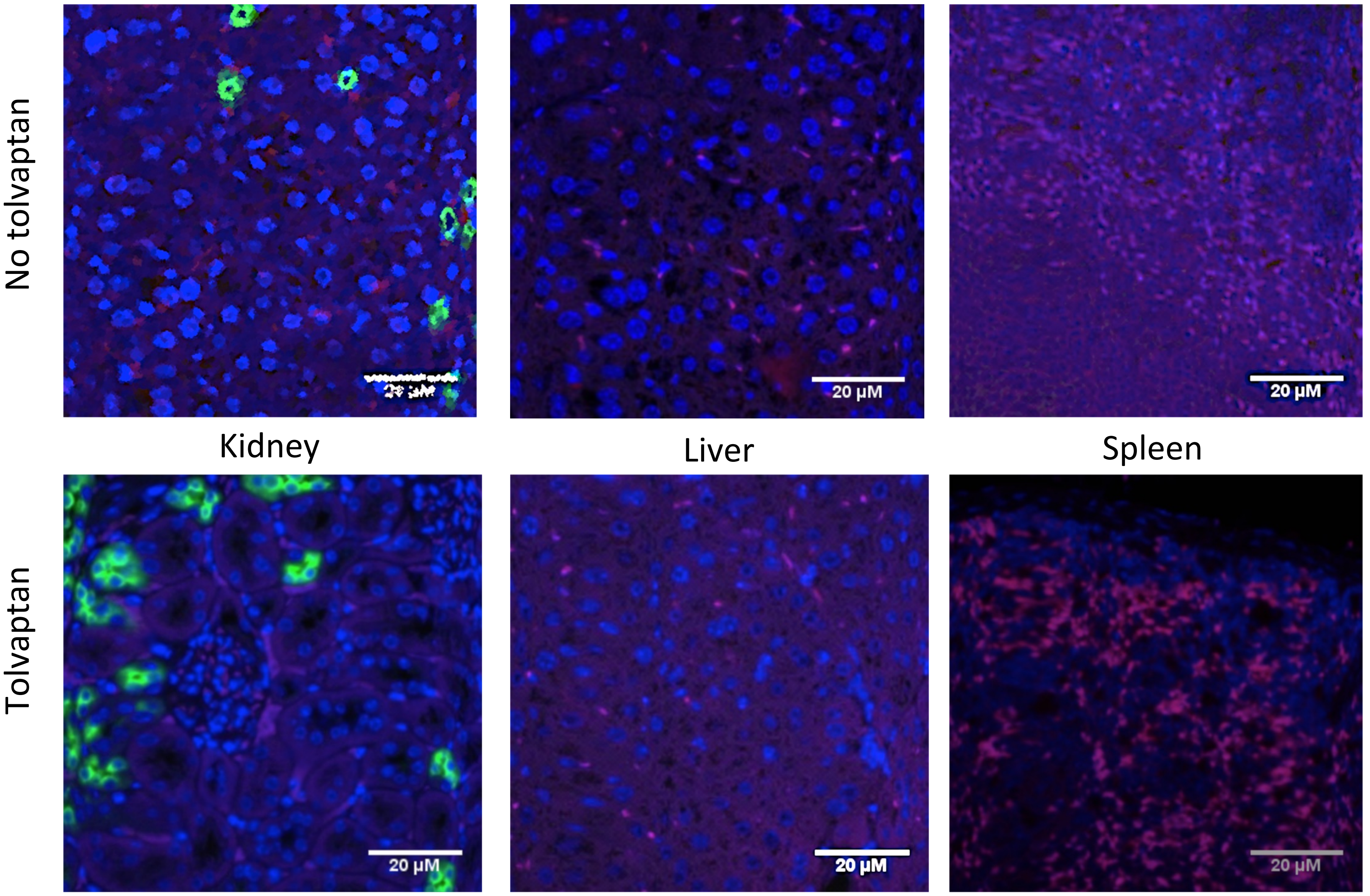
No tolvaptan
Tolvaptan
Kidney
Liver
Spleen
20 µM
20 µM
20 µM
20 µM
20 µM

Figure 8

Vasopressin regulates extracellular vesicle uptake by kidney collecting duct cells

Authors: Wilna Oosthuyzen, Kathleen M Scullion, Jessica R. Ivy, Emma E Morrison, Robert W Hunter, Philip J Starkey Lewis, Eoghan O'Duibhir, Jonathan M. Street, Andrea Caporali, Christopher D. Gregory, Stuart J Forbes, David J. Webb, Matthew A. Bailey and James W. Dear

Supplementary figure 1

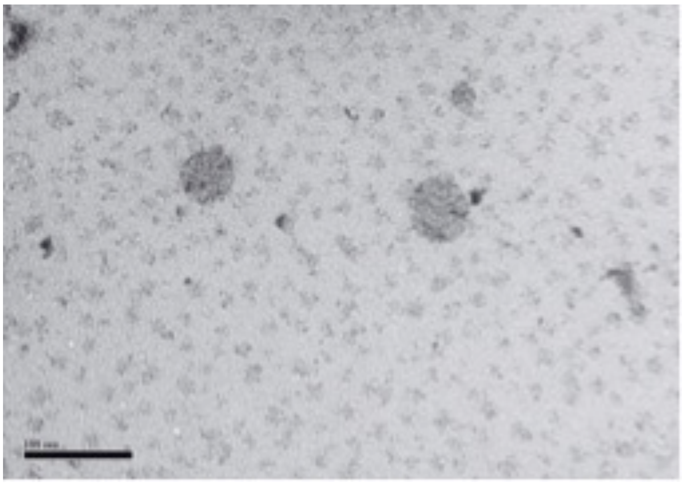

Supplementary figure 1. Structures of exosome size and shape are visible in the $mCCD_{C11}$ cell culture medium using transmission electron microscopy. Bar, 100 nm.

Supplementary figure 2

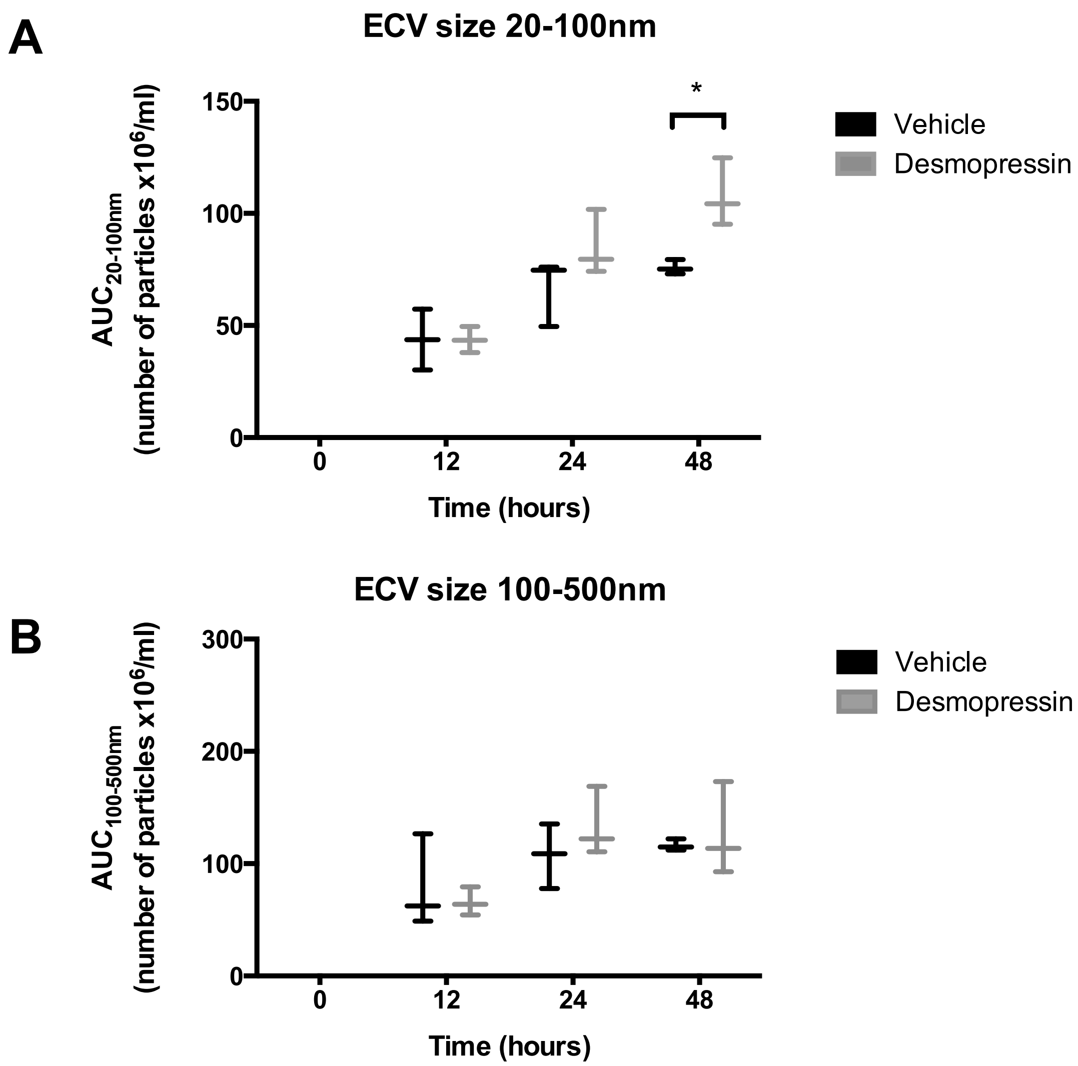

Supplementary figure 2. ECVs of exosome size are released from $mCCD_{C11}$ cells following stimulation by desmopressin. A) Number of particles in the supernatant from $mCCD_{C11}$ cells stimulated with desmopressin (3.16ng/ml) for the time indicated. Particles measured by NTA. Data are presented as the area under the concentration curve (AUC) for particles sized between 20-100nm. n=5. *p=0.02. B) Number of particles in the supernatant from $mCCD_{C11}$ cells stimulated with desmopressin (3.16ng/ml) for the time indicated. Particles measured by NTA. Data are presented as the area under the concentration curve (AUC) for particles sized between 100-500nm. n=5.

Supplementary figure 3

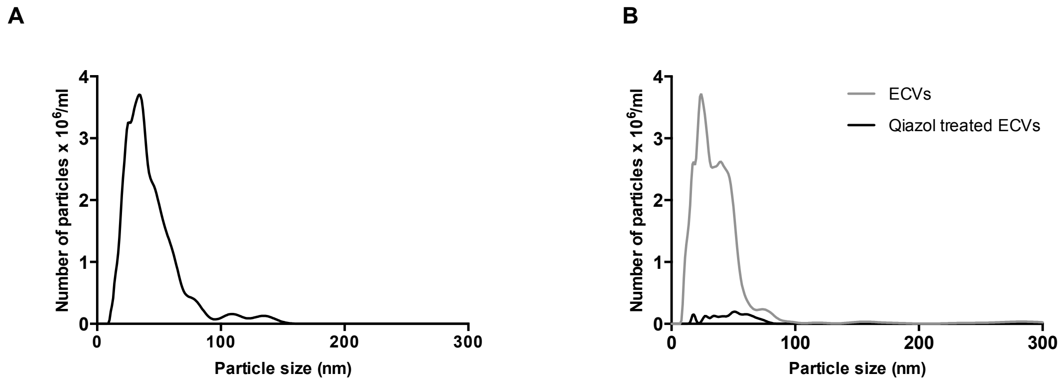

Supplementary figure 3. Kidney collecting duct cell ECVs were loaded with fluorescent Cell Tracker label and had an exosomal size distribution, as measured by NTA (A). Membrane disruption with QIAzol cell lysis reagent substantially reduced this NTA signal, consistent with fluorescent loading of membrane-bound ECVs (B).

Supplementary figure 4

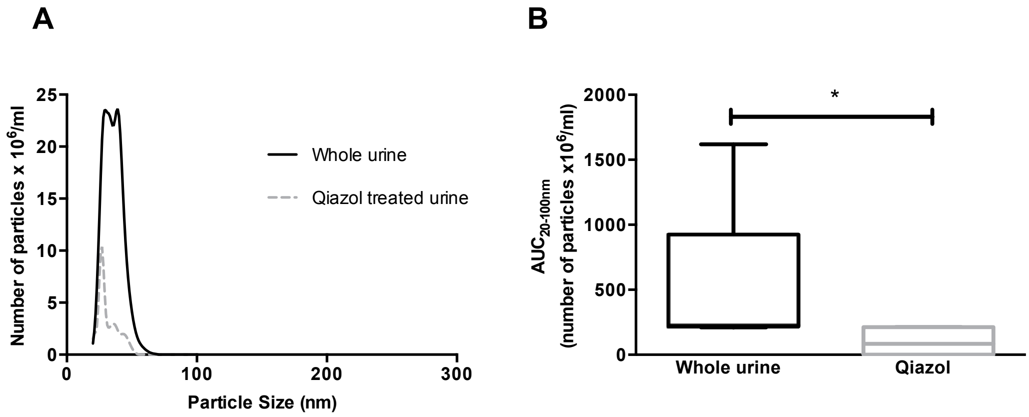

Supplementary figure 4. Particles of exosome size are present in mouse urine after intravenous injection of fluorescently-loaded ECVs derived from $mCCD_{C11}$ cells. Treatment of the urine with QIAzol cell lysis reagent substantially reduced this NTA signal, consistent with the presence of fluorescently-loaded membrane-bound ECVs. A). NTA trace demonstrating particle size and concentration. B) Tukey plot of urine before and after QIAzol treatment. Data are presented as the area under the concentration curve (AUC) for particles sized between 20-100nm. n=5. *$p<0.05$.